environments

MDPI

Article

Trends of Ocean Underwater Acoustic Levels Recorded Before, During, and After the 2020 COVID Crisis

Rocío Prieto González [1,2], Alice Affatati [1,3,4], Mike van der Schaar [1] and Michel André [1,*]

[1] Laboratory of Applied Bioacoustics (LAB), Universitat Politècnica de Catalunya-BarcelonaTech (UPC), 08800 Vilanova i la Geltrú, Spain; rocio.prieto.gonzalez@gmail.com (R.P.G.); aaffatati@ogs.it (A.A.); mike.vanderschaar@upc.edu (M.v.d.S.)
[2] Counting Whales, Rés Maeva Beach K5, Sainte-Luce, 97228 Martinique, France
[3] Department of Mathematics, Informatics and Geosciences, University of Trieste, 34128 Trieste, Italy
[4] National Institute of Oceanography and Applied Geophysics—OGS, 34010 Trieste, Italy
* Correspondence: michel.andre@upc.edu

Abstract: Since the Industrial Revolution, underwater soundscapes have become more complex and contaminated due to increased cumulative human activities. Anthropogenic underwater sources have been growing in number, and shipping noise has become the primary source of chronic acoustic exposure. However, global data on current and historic noise levels is lacking. Here, using the Listening to the Deep-Ocean Environment network, we investigated the baseline shipping noise levels in thirteen observatories (eight stations from ONC Canada, four from the JAMSTEC network, and OBSEA in the Mediterranean Sea) and, in five of them, animal presence. Our main results show yearly noise variability in the studied locations that is not dominated by marine traffic but by natural and biological patterns. The halt in transportation due to COVID was insignificant when the data were recorded far from shipping routes. In order to better design a legislative framework for mitigating noise impacts, we highlight the importance of using tools that allow for long-term acoustic monitoring, automated detection of sounds, and big data handling and management.

Keywords: passive acoustic monitoring; shipping noise; marine traffic; sound levels; cetacean presence; COVID-19; acoustic big data; Listening to the Deep-Ocean Environment

Citation: Prieto González, R.; Affatati, A.; van der Schaar, M.; André, M. Trends of Ocean Underwater Acoustic Levels Recorded Before, During, and After the 2020 COVID Crisis. *Environments* **2024**, *11*, 266. https://doi.org/10.3390/environments11120266

Academic Editors: Gaetano Licitra and Luca Fredianelli

Received: 13 October 2024
Revised: 3 November 2024
Accepted: 12 November 2024
Published: 22 November 2024

1. Introduction

Research studies have increasingly documented the extent and gravity of the risks humanity is facing and will face due to habitat and ecosystem depletion and degradation [1]. Large marine ecosystems are crucial in housing biodiversity and delivering valuable services and benefits. These coastal ecosystem services alone contribute US$125–145 trillion to annual economic worth, a substantial portion of the planet's overall economic value [2]. Nevertheless, human activities have significantly altered the oceanic environment, directly and indirectly, leading to increasing pollution and habitat modifications [3]. Pristine areas are becoming ever more scarce, with 41% of the world's oceans severely impacted by multiple drivers [4,5].

Among human-made stressors, underwater noise is widely recognized as a detrimental pollutant with potential long-term implications for marine ecosystems [3]. Over the last half-century, global shipping activity has increased, resulting in a twofold rise in ship traffic between 1950 and 2000 [6]. This surge in maritime transportation, coupled with the expansion of the global economy, has led to an escalation in underwater ambient sound levels (for example, at frequencies ranging from 10 to 100 Hz, at a rate of 3 dB per decade) [7–9]. Although this growth has slowed in recent years [10], research efforts on the impacts of anthropogenic noise levels on the marine habitat have increased. Shipping noise has been found to alter animal behavior and cause acoustic masking [11,12] and has been classified as chronic, i.e., "an unwanted acoustic signal that persists for a long duration without stable or predictable intervals" [13–16].

The COVID-19 pandemic slowed human activity globally ("anthropause", [17]). During the spring of 2020, various restrictions were imposed across the globe to tackle the virus outbreak. As economic activity decreased, the resulting slowdown in trade led to a 44% global reduction in marine traffic [18,19] with regional reductions in tanker vessels [20], fishing vessels [21], tourism vessels [22], ferries, and recreational vessels [19,23]. This slowdown in economic activities presented a unique opportunity for investigating changes in anthropogenic noise in several terrestrial (e.g., [24]) and marine (e.g., [25]) environments.

Several studies found reductions in underwater sound with decreases in low-frequency noise of 1.0 dB in the third-octave bands (TOBs), centered at 63 Hz off California [26], 1.6 dB (power density at 100 Hz) off British Columbia [27], 1.2 dB (10 Hz–1 kHz) in the German Baltic Sea [23], and 4.0 dB (111–140 Hz) off the Bahamas [28]. Changes in animal vocalizations have also been observed in response to noise reductions caused by the pandemic, such as a decrease in fish acoustic repertoire, or an increase in dolphin sounds detection (e.g., [29,30]). While several published studies have investigated changes in harbor areas close to shipping lanes, to the best of our knowledge, there is a lack of research targeting a global view of this phenomenon.

In this study, we explored acoustic data recorded by cabled networks at 13 sites distributed worldwide and corresponding to four marine areas, as shown in Figure 1. We aimed at investigating whether the reduction in sound pressure levels during COVID-19 was significant in different locations representative of diverse marine habitats, varying from the deep Pacific Ocean to the Mediterranean Sea, or the coast of the Northern Japanese island of Hokkaido. This wide selection of hydrophones included regions near shipping lanes and harbors as well as offshore areas, which may potentially have been less impacted by the reduction in shipping traffic. Depending on the location, data were analyzed from 2016 to 2021. The aim was twofold. Firstly, we examined the annual variability in noise levels and the reduction in sound pressure levels during the initial phase of the COVID-19 pandemic (January–April 2020).

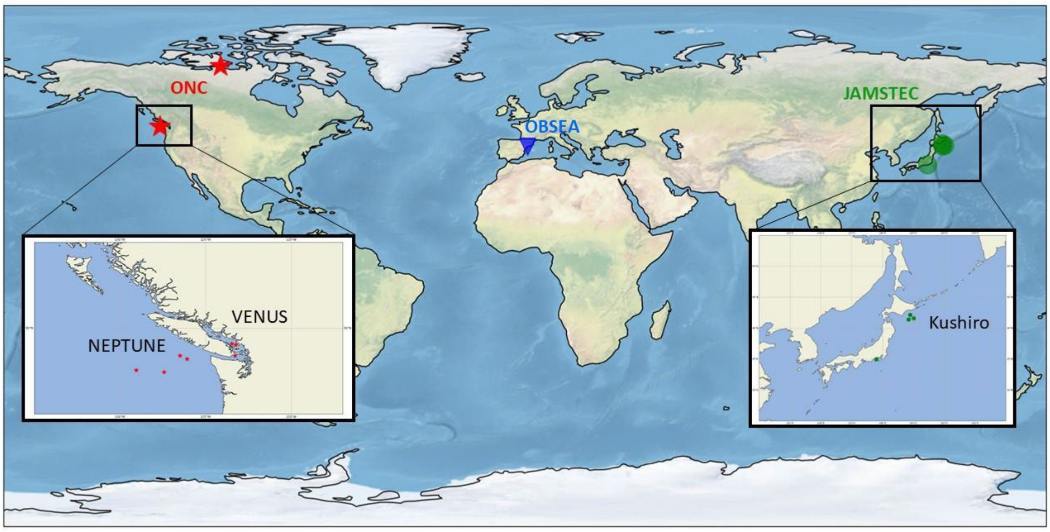

Figure 1. Locations of all the stations whose data we analyzed in the study. Red stars: ONC, Blue triangle: OBSEA, Green dots: JAMSTEC.

Additionally, we investigated the presence of cetaceans in the Pacific Ocean using their vocalizations as a proxy indicator for presence, even if the method may not always be accurate, as animals not vocalizing are ignored. Cetaceans were selected among other taxa since they indicate the health of a large variety of marine ecosystems [31,32]. Furthermore, some of the study areas included endangered cetacean species like the Southern Resident Killer Whales (*Orcinus orca*), which may be hampered by anthropogenic pressures such as ocean pollution, climate change, fishing, tourist activities, and marine traffic (e.g., [33,34]).

The data were managed through the online platform "Listening to the Deep-Ocean Environment" (LIDO, [35]) led by the Laboratory of Applied Bioacoustics (LAB) of the Technical University of Catalonia, BarcelonaTech (UPC). LIDO is one of the few web-based near real-time Passive Acoustic Monitoring (PAM) systems available [36] and is a useful tool for investigating and managing acoustic big data.

2. Materials and Methods

This work focuses on acoustic data analysis from thirteen sites collected by LIDO: the Expandable Seafloor Observatory (OBSEA; www.obsea.es; accessed on 20 November 2024) in the Mediterranean Sea, eight stations belonging to the Ocean Network Canada (ONC; www.oceannetworks.ca; accessed on 20 November 2024) (Endeavour, Clayoquot Slope, Barkley Canyon, and Cascadia Basin in the Northeast Pacific Ocean, Saanich Inlet and Strait of Georgia in the Salish Sea, Vancouver Island and Cambridge Bay in the Arctic Ocean), and four observatories in Japan, managed by the Japan Agency for Marine-Earth Science and Technology (JAMSTEC, www.jamstec.go.jp, three in Kushiro and one in Hatsushima; accessed on 20 November 2024) (Figure 1). The observatories were chosen from those available in LIDO, each with a minimum of two years of data, providing a broad overview that included hydrophones in shallow waters (as shallow as 6 m) and in the deep ocean.

2.1. Site Description

The OBSEA shallow water test site is a near real-time cabled seafloor observatory located 4 km off the coast of Vilanova i la Geltrú (Barcelona, Spain) in a fishing-protected area on a narrow continental shelf. Its omnidirectional digital hydrophone recorded a broadband range of frequencies (5 Hz to 300 kHz) with a gain set to 20 dB, a quantization range of ±2.5 V, and a typical sensitivity accuracy of ±3 dB. All the files were in a 16-bit format.

ONC is a network managed by the University of Victoria that monitors the West and East coasts of Canada and the Arctic. Operating remotely, these observatories continuously gather near-real time open access data available for scientific research.

Firstly, among the Northeast Pacific Time-series Underwater Networked Experiments (NEPTUNE) observatory, we analyzed data recorded by Barkley Canyon, Cascadia Basin, Clayoquot Slope, and Endeavor. NEPTUNE nodes are located off the West coast of Vancouver Island around the Cascadia subduction zone in areas with soft, muddy sediments 3–5 km thick. Despite the high pressure and temperatures below 2 °C, a variety of deep-sea organisms live in the area, attracting fish and marine mammals. The Endeavour region is part of a complex major hydrothermal vent environment. The Main Endeavour Vent Field (MEF) is located between the Juan de Fuca and Pacific tectonic plates, while Mothra is located about 3 km south of MEF in the axial valley. Secondly, the Saanich Inlet and the Strait of Georgia belong to the Victoria Experimental Network Under the Sea (VENUS). The Saanich Inlet is a glacial fjord with low currents and a variable sea bottom composition. The Strait of Georgia is located at the Fraser River delta and is swept by a variable tidal current. Finally, we investigated the Vancouver Island site, which is enclosed by the inner coastal waters of the Salish Sea and the Pacific Ocean, and the Cambridge Bay node, located in the Arctic region, in the Nunavut territory.

For all ONC nodes, calibration curves were provided by the ONC, accounting for the digitization of the data (sensitivity of the hydrophone, gain, quantization). At all stations, the hydrophone sensitivity used was the mean of the sensitivities along the frequencies of interest, and all the files were in a 24-bit format.

JAMSTEC maintains a network of hydrophones dedicated to aid in earthquake studies for disaster mitigation around the Japanese islands. The Kushiro cabled observatory has four hydrophones and three ocean-bottom seismometers located at the landward slope of the southern Kuril subduction zone. The Hatsushima hydrophone is part of a multidisciplinary observatory that monitors geophysical and biological phenomena and seismic activities. The hydrophones use their own format, where data are received in a 32-bit format and then decoded following JAMSTEC documentation.

Technical characteristics of the hydrophones belonging to the selected nodes (locations, characteristics, and recording time period; see Figure 2) are shown in Supplementary Table S1.

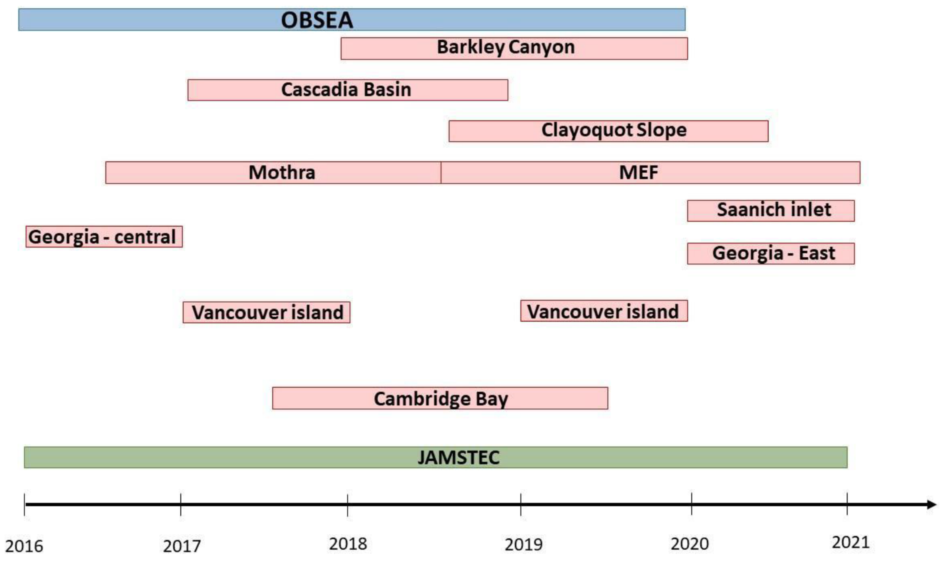

Figure 2. Available data recordings from 2016 to 2021 for the selected stations. The same color code indicates nodes belonging to the same network: OBSEA in blue, ONC in red, and JAMSTEC in green.

2.2. Data Analysis

The data were analyzed for two different purposes. First, the variability in noise levels was evaluated, allowing us to assess the potential global pause of marine traffic at the start of the COVID-19 pandemic. Second, a methodology for detecting animal presence was developed. In both cases, the methodology was adapted to the specific site depending on the characteristics and availability of the data. The statistical analysis was conducted using R software, version 4.3.1 [37].

2.2.1. Noise Levels

To evaluate changes in noise levels before and after the onset of the COVID-19 pandemic, a band capturing shipping noise contributions, referred to as the shipping noise band (SNB), combining TOBs from 63 to 125 Hz, was compared during the first four months of 2020 and the corresponding period in previous years at each location. Because OBSEA and JAMSTEC data had already been processed by LIDO, the SNB definition was set to fit the available frequency bands. For OBSEA, the LIDO processed output included noise measurements (peak and rms signal levels) across the entire frequency spectrum, rms noise in four frequency bands, detection of impulses, and short tonal events. Consequently, the OBSEA SNB was defined as the sum of TOBs centered at 63 and 125 Hz. However, raw data from the ONC network were specifically processed for this study, with all TOBs from 63 to 16,000 Hz computed. Therefore, the SNB was determined as the sum of the TOBs centered at 63, 80, 100, and 125 Hz. In the JAMSTEC network, systems were sampled at 100 Hz, since they were focused on the low-frequency earthquake sounds. The processed output consisted of noise measurement (rms signal levels) over the whole frequency band, an impulse detector, and sound levels associated with two frequency bands ranging from 5 to 45 Hz and 15 to 25 Hz. Hence, the SNB was defined as the frequency band from 5 to 45 Hz.

ONC wav files were downloaded using a Python script [38]. For all stations, except Vancouver Island, three 5 min files were saved every hour, evenly spaced in time to cover consecutive intervals. For Vancouver Island, two 5 min wav files per hour, separated by half an hour, were downloaded. The sound pressure level in TOB was computed using a Butterworth filter with a 10 s time window, as suggested in the JOMOPANS guidelines [39].

Patterns in the annual SNB variations of the sound pressure levels were analyzed. The goal was to discover if the traffic decline during the emergency state due to COVID-19 had a significant effect, regardless of changes in level that might be associated with shifting hydrophone sensitivities and any other variations.

Trends of the OBSEA SNB levels during the first months of each year from 2017 to 2020 were examined. Data from 2019 was excluded from the analysis, due to data gaps. A visual inspection revealed that each year began with a significant increase in SNB levels, followed by a single major decrease. To compare the drop rate between years, we manually selected the timing of these drops: from February to May 2017, April to July 2018, and February to May 2020.

For ONC and JAMSTEC, when data from 2020 were included in the data set, the first four months of each year—from January to April—were selected to compare the trend of the SNB levels. From this point on, the methodology followed the same steps at all locations. The data dimension and its variability were reduced by taking the daily median of the SNB levels. A linear model of the daily median of the SNB levels was fitted in the selected period, and the 95% confidence bands were estimated. To ensure a fair comparison of the linear model across years, the SPL data were normalized by indexing each year to May of that same year. The median SPL value from the first week of May was subtracted for every year—a week that all years shared during the decreasing trend period—to reduce the effect of the different hydrophone calibrations and their sensitivity variations, creating a relative measurement. Then, a 30-day moving window was used to calculate the slope of the SNB levels for each window and to create a slope distribution. Other window lengths (7 and 15 days) were also tested. Since no significant differences were found across these varying window lengths, the 30-day window was chosen to focus on capturing longer-term trends rather than daily fluctuations.

The yearly slope distributions and the mean (and median) were compared between years to assess whether there was a significant decrease in 2020 SNB levels for each location (and thus a significant effect in 2020, related to the global shipping disruption caused by the pandemic). When the normality assumption held, parametric tests with more statistical power, such as t-test or the one-way analysis of variance (ANOVA), were applied. By contrast, when the normality assumption did not hold, the Kruskal–Wallis test by ranks, the Mann–Whitney U test, and the Kolmogorov–Smirnoff tests were computed. The Bonferroni correction was applied as a p-value adjustment to compare multiple years.

2.2.2. Animal Presence

The analysis of animal presence focused on cetacean vocalizations. At OBSEA, cetacean vocal activity was minimal, with invertebrates being the primary biological contributors [40]. Consequently, cetacean presence was assessed only at the ONC and JAMSTEC observatories. The methodology used was tailored to the location, since the selected species have different acoustic repertoires and vocalize at different frequencies. The analysis for both main areas is described in the following subsections.

ONC

Cetacean presence was investigated for Endeavour, Barkley Canyon, Clayoquot Slope, and Vancouver Island. Stations were selected where the presence of animals was more likely given the characteristics of their location (e.g., bathymetry, prey availability) A pilot analysis and the consequent methodology development was implemented using data downloaded from the Endeavour node, chosen because of its considerable distance from harbor. The analysis was conducted using LIDO, which has an interface that allows choosing the date, sensor, and detector, but also visualizes indicator values (normalized sound levels values; [36]) and the relative spectrograms. In order to be consistent with the evaluation of SNB levels, the first four months of each year—from 2017 to 2020—were studied.

The sensors analyzed were "Endeavour Mothra vent" for 2017–2018 and "Endeavour Mothra periodic" for 2019–2020. Five detectors were examined: (a) two short tonals (1–2500 Hz and 2500–20,000 Hz) and (b) three impulse detectors (100–500 Hz, 500–5000 Hz, and 5000–20,000 Hz). Short tonal detectors aimed to pick a strong energy signal near the hydrophone. Hence, whistles and baleen whale harmonics, but also chain noise, vessels, or other tonal sounds could trigger these detectors, while impulse detectors mainly targeted sperm whale (*Physeter macrocephalus*) cues.

For each detector, we systematically scanned the indicator values, scaled between 0 and 100, at 24 h intervals, setting a minimum threshold of 10 and excluding data below this threshold. Spikes above the overall trend of the baseline level were checked. Animal presence was assessed by zooming at a finer time resolution and checking the spectrogram visually and acoustically. However, exceeding the baseline level did not necessarily indicate the presence of an animal; it could potentially be a false positive case caused by other triggering sources. In 2017, for the short tonal 1–2500 Hz and in 2018, for the impulses 5000–20,000 Hz, a Receiver Operating Characteristic (ROC) curve was generated. The ROC illustrates the diagnostic ability of a binary classifier system between sensitivity and specificity for various thresholds. We identified the threshold that removed false positives, ensuring that all detections above this level were true animals without needing correction. However, this systematic approach did not yield sufficient cetacean detections for further analysis across the years.

After the Endeavour pilot analysis, a new methodology was developed for detecting cetaceans in the remaining locations. This methodology involved a less extensive manual checking process, which resulted in faster data processing. Improvements were made in treating the data from Endeavour, automatically selecting the peaks above the baseline level instead of manually. Indicator values from the detectors were smoothed using a moving average of a ten-sample window. The smoothed indicators were processed to find the time of the local maxima linked to a possible threshold, which resulted in a distribution of smoothed thresholds. The 99th percentiles for the short tonal and the 95th percentiles for the impulse detector were selected. The percentile for the short tonal detector was chosen so that the vocalization of target animals would present more than 1% of the time during the 10s spectrogram segment. However, this scenario is unlikely for a strong whistle or harmonics in a baleen whale call. In the impulse detector case, the threshold was set lower but remained conservative since vessels triggered the detector less frequently and sperm whales were present more than 1% of the time. A second improvement involved selecting a random sample of n = 30 segments that exceeded the respective threshold for each year and detector. Through LIDO, an associated link was produced for each of these segments to reproduce it online. Segments were then visually and acoustically analyzed in search of cetacean presence. The aim was to estimate the false positive rate to compare the animal cue detections across years. All years were pooled together for each detector and location to increase the sample size and have a more robust estimate. Animal detection percentages were estimated yearly by location for each detector, corrected by the false positive rate.

Locations were selected based on prior information about cetacean presence and bathymetry. For Barkley Canyon and Clayoquot Slope, six detectors were examined: three short tonal (1–2500 Hz and 2500–20,000 Hz, and 20,000–46,000 Hz) and three impulse bands (500–5000 Hz, 5000–20,000 Hz, and 20,000–46,000 Hz). Meanwhile, two short tonals (1–2500 Hz and 2500–20,000 Hz) and two impulse bands (500–5000 Hz and 5000–20,000 Hz) were available for Vancouver Island.

JAMSTEC

Ocean-bottom seismometers have a low sampling rate, which limits their use for monitoring the low-frequency calls of baleen whales. They are particularly suited for investigating fin whales (*Balaenoptera physalus*) and blue whales (*Balaenoptera musculus*) that, emit sounds below 45 Hz. Animal presence was studied for Kushiro Observatory 1. We followed the same improved methodology from ONC. The short tonal 10–45 Hz detector was analyzed to estimate the false positive rate and, hence, the estimation of the cetacean presence.

3. Results

Due to the size of the analysis, only the results computed for some locations are presented in the main paper, while the others can be found in the Supplementary Information.

3.1. Noise Levels

In general, the SNB levels followed a site-dependent yearly periodic pattern. This annual variation of the sound levels was observed across nearly all SNB locations, although the specifics varied from one site to another in terms of trends, variability, and frequency. The annual average SNB level from all stations examined fluctuated around ±7 dB. The minimum and maximum values observed were 77 and 128 dB re 1 μPa^2, respectively. The lowest SNB levels, ranging from 77 to 90 dB re 1 μPa^2, were recorded at the OBSEA site (Figure 3), while the highest were detected at Hatsushima, reaching levels of up to 128 dB re 1 μPa^2 (Supplementary Figure S1j).

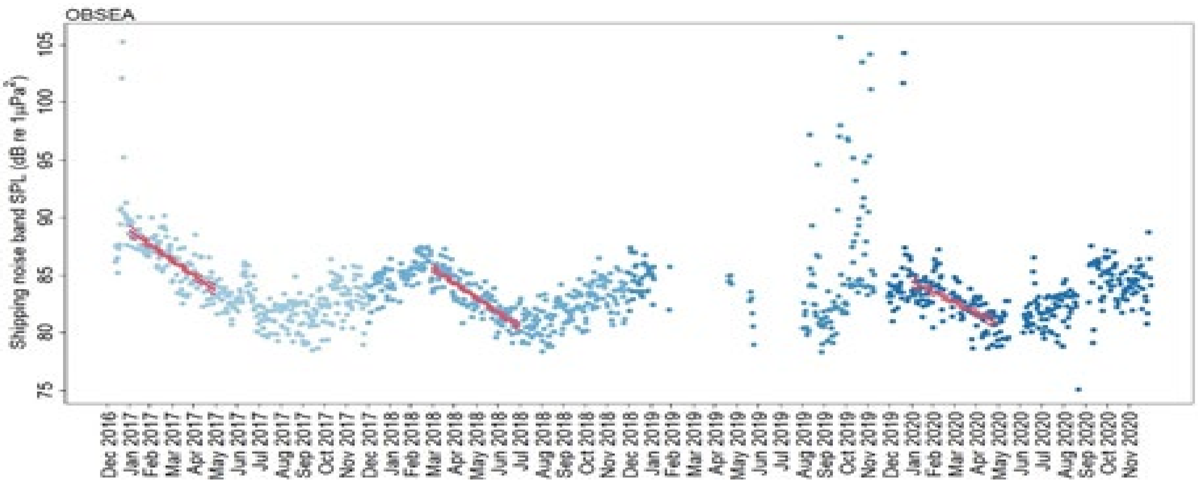

(**a**)

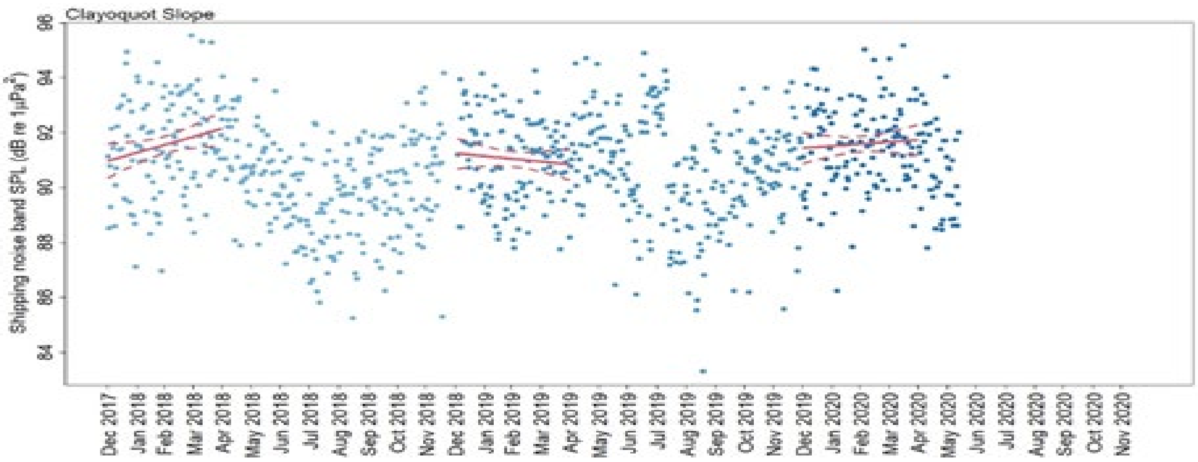

(**b**)

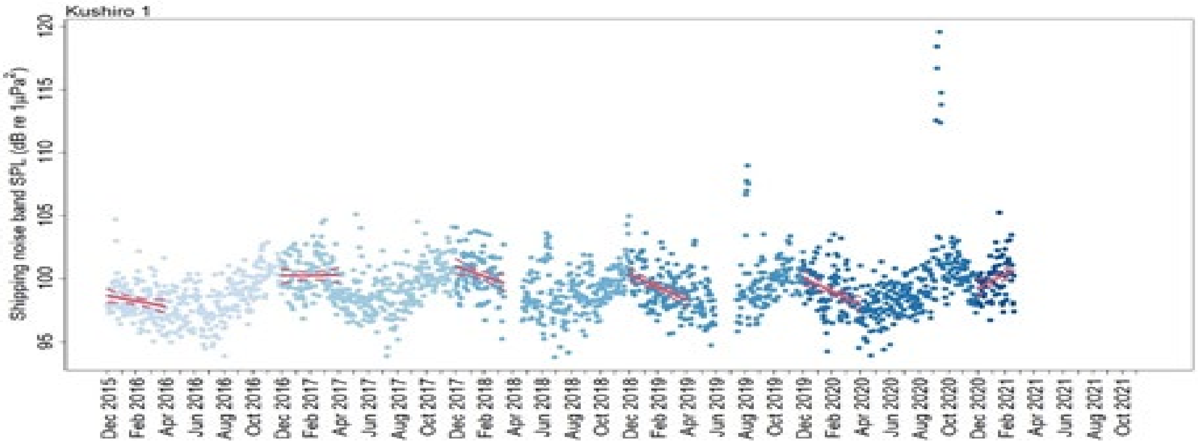

(**c**)

Figure 3. Shipping noise band daily median for (**a**) OBSEA (from 2017, 2019, and 2020), (**b**) Clayoquot Slope (from 2018 to 2020), and (**c**) Kushiro 1 (from 2016 to 2021). Blue dots represent the daily median values, with colors transitioning from light to dark blue by year. The linear model fitted to each selected period by year is the red solid line and the red dashed lines are the 95% confidence intervals.

There were two exceptions, Saanich Inlet and Cambridge Bay, where there was an increase in yearly variability of approximately ±20 dB (Supplementary Figure S1d,g). The SNB levels showed an annual periodic trend with a near half-year cycle of decreasing, followed by increasing, levels across most of the locations, including OBSEA, Barkley Canyon, Cascadia Basin, Clayoquot Slope, Endeavour, Vancouver Island, and all Kushiro sites (Figure 3; Supplementary Figure S1a–c,f,h,i). The decreasing period typically started at the beginning of the year, between January and March, followed by a rise in noise levels at the end of the year. However, identifying an annual pattern in Saanich Inlet proved challenging due to the limited data available for only a single year, with minimal data and high variability (Supplementary Figure S1d). Nevertheless, a rise in noise levels was observed during the beginning of the only year of data (Supplementary Figure S1d).

In the Strait of Georgia, the pattern consisted of two consecutive decreasing periods with a short pause in June (Supplementary Figure S1e). This pattern was similar in both years despite showing an increase in absolute values of 10 dB from 2016 to 2019, possibly due to different hydrophone configurations. At the Arctic station, there was an increase in variability in 2019, but it seemed that the trends and fluctuations were repeated, changing the scale of dispersion (Supplementary Figure S1g). Similarly, in Hatsushima, the same effect was seen in both adjacent years. A three-step function described the SNB levels pattern with flat, decreasing, and increasing intervals, although in the second year, there were higher jumps due to the rise in variability (Supplementary Figure S1j).

During the COVID-19 period, three main behaviors were observed compared to other years. First, a decreasing period was visible in OBSEA, Endeavour, Strait of Georgia, and Kushiro 1 and 2. The rate of the drop was similar during all years in OBSEA and in Endeavour. In OBSEA, the drop followed a general decreasing trend over time (Figure 3a), while in Endeavour, there was a fluctuation, reaching the highest values in 2019 (Supplementary Figure S1c). In the Strait of Georgia, SNB levels exhibited a steep drop in 2016 and a gentler decline in 2019 (Supplementary Figure S1e). In Kushiro 2, a slight fall was observed from 2016 to 2018, but no data were available for 2019. In 2020, there was a sharp decrease in SNB levels, followed by growth the following year (Supplementary Figure S1h). Second, a stable pattern can be seen in Cascadia Basin, Kushiro 3, and Hatsushima, despite insufficient data in 2019 (Supplementary Figure S1b,i,j). This constant trend sometimes incorporated a gentle decline, as seen in Cascadia in 2019 (Supplementary Figure S1b). Third, a fluctuation between years with different trends was observed in the mentioned period. In Barkley Canyon, SNB levels declined in 2019, but showed growth at the start of 2020 (Supplementary Figure S1a). In Clayoquot Slope, there was a rise in 2018 SNB levels, followed by a marked fall during 2019 and a return to a steady rise in the following year (Figure 3b). By contrast, in Vancouver Island, although it was difficult to see a common pattern at the beginning of the year, the main SNB levels trend decreased in 2017 and increased in 2019 (Supplementary Figure S1f). The yearly distribution of shipping noise band daily medians, along with the daily averages, is presented in Supplementary Figure S3.

To sum up, looking at the slope distribution of SNB levels, we saw a decrease in sound levels during the COVID-19 year at Barkley Canyon, Cascadia Basin, Clayoquot Slope, Endeavour, Strait of Georgia, and Kushiro 1 (Figure 4; Supplementary Figure S2a–d).

In some locations, a drop can be expected during the first few months of the year as part of the usual variation in sound levels. In other words, similar periodic fluctuations were observed in previous years. For instance, the slope of the SNB levels for Cascadia was steeper during 2019 than in the other years (Supplementary Figure S2b), while in Clayoquot Slope and Kushiro 1, the average SNB levels were the lowest (Figure 4). Moreover, a consistent decreasing trend over time was observed in OBSEA. Therefore, the slope distributions of SNB levels for each year were compared to quantify differences in steepness, to determine whether there was a significant change related to the shipping slowdown in 2020 at each location.

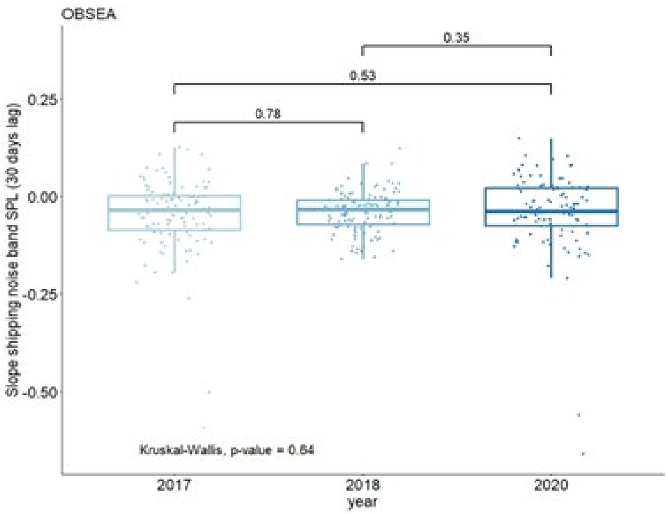

(**a**)

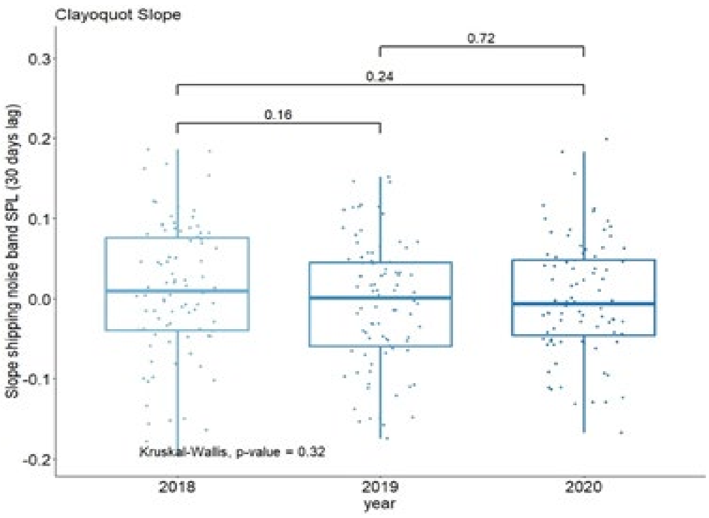

(**b**)

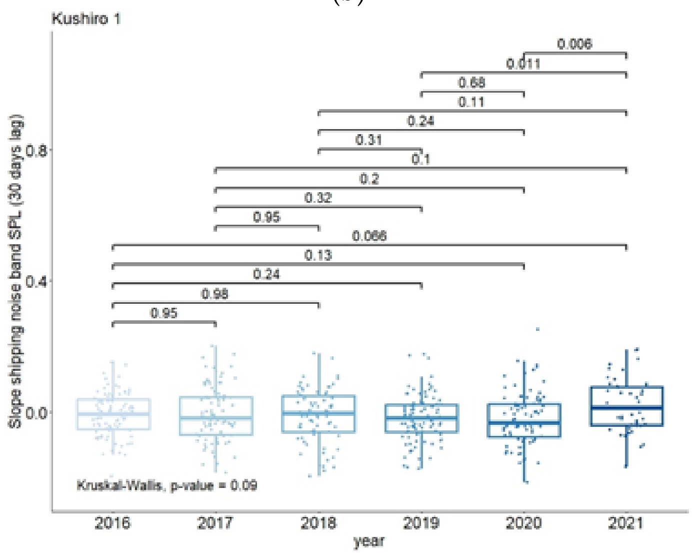

(**c**)

Figure 4. Slope distribution (one month lag) of shipping noise band levels daily median per year during the selected period for (**a**) OBSEA, (**b**) Clayoquot Slope, and (**c**) Kushiro 1. Individual observations on top of boxes were added by shifting all dots by a random value to avoid overlaps. The median comparison *p*-value of the pairwise Wilcoxon test is displayed on top of the box plots and the *p*-value of the Kruskal–Wallis test , comparing multiple years.

Based on the *p*-values of the Shapiro–Wilk test for normality (Supplementary Table S2) for OBSEA, Endeavour, Cambridge Bay, Kushiro 3, and Hatsushima, the assumption of normality was rejected with 95% confidence in at least one year. For the remaining locations, no significant departure from normality was found. Subsequently, a one-way ANOVA was applied to Clayoquot Slope and Kushiro 1 and 2. For Kushiro 2, the observed *p*-values were less than 0.05, indicating enough evidence to conclude that the means of the slope were significantly different from the others in at least one of the years (Supplementary Table S3). The t-test revealed a significant difference between the means of the slope SNB levels' daily median distribution in the Strait of Georgia, Vancouver Island, and Kushiro 2 (Supplementary Table S4).

If we examine the Kruskal–Wallis test (Figure 3; Supplementary Figure S2c,g,h, and Table S5), we see that the null hypothesis (which means that the population medians are all equal) was only rejected for Kushiro 2. Thus, reaffirming the ANOVA results, at least one of Kushiro's two years likely originated from a different distribution than the others. In particular, at Kushiro 2, the rate of drop in the daily median of SNB levels appeared to be lower in 2020 compared to other years (Supplementary Figure S2g). However, based on the t-test Bonferroni correction *p*-values, the difference was only significant between 2020 and 2021. Moreover, this was the only location where a significant difference was observed in 2020 (Supplementary Table S4).

The Wilcoxon test, which considers a null hypothesis of pairwise equal medians, concluded at a 5% significance level that the slope SNB levels distribution in the Strait of Georgia, Vancouver Island, Kushiro 1 and 2, and Hatsushima were non-identical (Figure 3; Supplementary Figure S2a–i, and Supplementary Table S6). The Wilcoxon test does not assume that the data are sampled from a Gaussian distribution. However, it does assume that the data are distributed symmetrically around the median. Nevertheless, the Kolmogorov–Smirnov test covers the more flexible case of asymmetrical distributions. In addition to the Strait of Georgia, Vancouver Island, Kushiro 1 and 2, and Hatsushima, for Endeavour and Cambridge Bay, the null hypothesis that the two samples were drawn from the same distribution is rejected with 95% confidence, i.e., the slope SNB levels distribution was significantly different (Supplementary Table S7), and that difference was only significant in 2020 at Endeavour, Kushiro 1, and Kushiro 2, compared to 2018, 2021, and 2021, respectively.

3.2. Animal Presence

3.2.1. ONC

Three cetacean species were identified in the ONC observatories: humpback whales (*Megaptera novaeangliae*), killer whales (*Orcinus orca*), and sperm whales (*Physeter macrocephalus*). Impulse detectors primarily picked up sperm whale clicks and sporadic killer whale cues, while humpback and killer whale vocalizations were detected through the short tonal detectors. Killer whale detections were consistently lower in all locations compared to humpbacks and sperm whales.

In Endeavour, the results for the manual checking for each detector from January to April 2018–2020 are summarized in Supplementary Table S8. The ROC curve for the impulse 5000–20,000 Hz detector in 2018 (Supplementary Figure S4) illustrates the diagnostic ability of the detection model to identify a variation in the threshold. However, the limited presence of cetaceans hindered the application of this approach over the years. In Barkley Canyon, Clayoquot Slope, and Vancouver Island, the false positive rate was estimated based on the selected thresholds for each detector per year (Supplementary Tables S9, S10, S12, S13, S15, S16). To illustrate how the random links were created, an example for all detectors in Barkley Canyon 2019 is shown (Supplementary Figures S5–S10).

The percentage of time an animal vocalization was above the selected threshold, corrected by the false positive rate, was estimated for each detector annually. In Barkley Canyon, there was an increase in the number of detected animals in 2020 for the short tonal ranges of 1–2500 Hz and 20,000–46,000 Hz. By contrast, at the short tonal 2500–20,000 Hz detector and the impulses detector between 20,000–46,000 Hz, there was a decrease in animal detection through the three consecutive years, while the other detectors remained stable from 2018 to 2020 (Supplementary Table S11). In the Clayoquot Slope, the number of detected animals decreased from 2018 to 2019 across all detectors, except for the impulse detectors between 500–5000 Hz and 5000–20,000 Hz (Supplementary Table S14). A similar trend was observed in Vancouver Island, where the percentage of detected animals decreased from 2017 to 2019, except for the short tonal 2500–20,000 Hz detector (Supplementary Table S17).

3.2.2. JAMSTEC

Only one detector, the short tonal 10–45 Hz, was considered in the Kushiro 1 observatory to detect fin whales' calls, since these animals can be found around the coast of Japan. The selected thresholds per year (Supplementary Table S18) were used to estimate the false positive rate (Supplementary Table S19). The percentage of animal detection, adjusted for false positive rates, showed a peak of 6% in 2016, fluctuating between 1% and 1.5% from 2017 to 2021 (Supplementary Table S20).

4. Discussion

We investigated the yearly variability of SNB levels in 13 locations and the change, or drop, in sound pressure levels during the initial phase of COVID-19 in Europe from January to April 2020. As a parallel effort, animal presence was investigated using data gathered from PAM in five observatories in the Pacific Ocean.

Our initial motivation was to assess whether the maritime lockdown due to COVID-19 affected SNB levels at three locations. While we did not observe direct effects from changes in shipping activity, a significant annual and seasonal variability was identified in the frequency bands considered. This led us to expand the study to additional locations, providing a broad overview, to determine whether similar patterns were present across other regions as well.

Recent studies have highlighted reductions in sound levels in marine environments during the COVID-19 pandemic in the Pacific Ocean and the Baltic Sea in Europe [18,23,26–28]. However, these studies focused on data collected from recording systems positioned near shipping lanes or harbors, displaying a more significant impact from halts in shipping traffic compared to more offshore areas, like those we investigated. In this study, we analyzed sound levels at six coastal observatories and seven offshore ones. Our main findings align with what other authors found. For example, in Sarasota Bay (Florida), vessel activity increased during the COVID-19 period by almost 80% at one of their studied sites and remained the same at the other site [41]. Moreover, [42] found that sound levels decreased in 2020 along the southeastern United States shelf break waters, although these changes were unrelated to the COVID-19 slowdown.

Underwater environments are dynamic and experience variability in sound propagation in space and time. Our findings suggest that there is a yearly variability in SNB. Between 1965 and 2003, the number of commercial vessels approximately doubled, the gross tonnage quadrupled, and the horsepower increased [43]. Thus, the ongoing increase in commercial shipping could result in an overall upward trend in SNB levels. A decrease in the number of vessels present in 2020 compared to 2019 was noticeable [19,42]. While there may have been a reduction in shipping noise levels concentrated in anthropized areas during the first months of restrictions, we argue that, in the specific locations we examined, sound reductions of the “COVID-19 magnitude” occur every year, particularly early in the year. Despite this, in most locations, this decrease in sound levels was not statistically significant between 2020 and other years.

Sound level variability has been observed by other researchers as well. For instance, [44] studied fluctuations in the received levels of vessel noise in the Juan de Fuca Strait. They found significant variability, with temporal differences between 3 and 5 dB due to seasonal temperature changes resulting in varying water masses and daily tides. Another study on underwater sound monitoring in the Baltic Sea [45] discovered a nearly 50 dB difference in the 63 Hz one-third octave band while comparing the annual median sound pressure level of the quietest and the loudest locations. The authors suggested that the sound seasonal variability of the Baltic Sea is mainly related to periodic variations in the sound speed profile along the water column. Data collected at the Bornholm Deep and at the Gdansk Deep (Southern Baltic Sea, in winter and summer, respectively), two areas with different sound propagation conditions, was analyzed in [46]. The noise spectrum levels indicated a strong dependence on seasonality, location, and depth of sound sources. Various environmental factors can influence this variability, including biotic, abiotic, and anthropogenic factors. Our study encompassed various environmental conditions and levels of ship traffic intensity. Understanding this variability is crucial for estimating changes in acoustic environments and their potential effects on marine fauna [44].

In the selected locations, the observed annual and seasonal variability in SNB levels appears to be unaffected by the reduction in marine traffic, even when focusing on those specific frequency bands. This suggests that biophony and geophony may be the main contributors. Unfortunately, data from the Strait of Georgia, where vessel noise, primarily from ferries, predominates, was unavailable during the COVID period, preventing a comparison of the pandemic's effect across years. However, a significant difference in SNB levels between 2016 and 2019, the only two available years, was observed. In many open ocean locations, the soundscape may be dominated by noise from distant and local storms. Meanwhile, sheltered locations like OBSEA, Saanich Inlet, or Cambridge Bay could be influenced by small boat activity, although no significant effects were detected. At OBSEA, the soundscape was largely dominated by invertebrates, the primary biological contributors [40], while at Cambridge Bay, snowmobile noise could be a possible source of contribution. The seasonality in SNB variations seems to be driven by the sea state, with noise increasing in winter and decreasing in summer. The reduction in storm activity during spring may also explain the decreasing noise trends observed in that period.

Based on the current study, we cannot definitively conclude that the soundscape is dominated by any particular source without conducting a more in-depth analysis. However, our findings indicate that the variation in SNB levels was not primarily driven by marine traffic, suggesting instead a dominance of natural and biological sounds. This implies that the selected data may not serve as a reliable proxy for shipping noise for these specific observatories. In addition, the analyzed locations differed in oceanographic characteristics, including bathymetry, sediment composition, and water depth, all factors that can affect underwater sound propagation. The location of a hydrophone and its position within the water column can also significantly impact the recorded data, with bottom-mounted hydrophones yielding different results compared to those suspended in the water column. The aim of each study drives the design of different hydrophone positioning in an area or hydrophone array configurations.

We investigated cetaceans' presence at the ONC and JAMSTEC stations. These animals are often wide-ranging and are found in several habitats, from shallow coastal waters to abyssal canyons. Cetaceans can migrate between areas rich in food and areas suitable for reproduction. For example, many mysticetes seasonally feed in food-rich areas in the polar summer and migrate over long distances to sub-tropical areas in winter for mating and birthing. For these reasons, they are exposed to many anthropogenic stressors, including collisions with vessels and underwater noise pollution (e.g., [47,48]).

Vocalizations of humpback whales, killer whales, and sperm whales were detected in the ONC observatories, indicating this method's potential in detecting vocal animals. The lack of cetacean presence near the Endeavour hydrophone, situated far from the coast, was expected. On the other hand, hydrophones in Barkley Canyon, Clayoquot Slope, and Vancouver Island are deployed in locations known for the presence of cetaceans. We expected that the COVID-19 restrictions would result in a decline in recreational boating activity and consequent ambient noise levels, thereby prompting an increase in the detection of cetaceans potentially due to diminished vessel disturbances (e.g., [49,50]).

Regarding the observatories in Japan, our research mainly focused on Kushiro 1, where we investigated fin whale vocalizations. The sound produced by these cetaceans, vocalizations around 20 Hz, is a significant component of the soundscape of this region. In the particular case of the Kushiro observatory, an increase in fin whale presence might cause an increase in sound level measurements when 20 Hz is included in the measurement band [51]. Fin whale call sequences are geographically distinct and unique to a population [52], and their rhythm can be synchronized and modified over extended periods of time. For example, there was a sudden change in the type of fin whale call observed in California during the period investigated by [53]. Sometimes, populations coexist temporally and spatially, leading to songs overlapping. Research on fin whale calls has revealed seasonal variations in ambient noise spectrograms of continuous long-term waveform records. In Japan, this seasonal pattern resulted in high-intensity signals from September to February over cold winter months at higher latitudes [54]. Similar patterns were found along the Chilean coast, with minimal to no songs during the Austral summer and an increase in song occurrence in the Austral winter [55].

Due to the expansion of technical capabilities and the development of associated software, signal detection and classification techniques have evolved. The advantage of using algorithms for automated signal detection is that it significantly reduces analysis time and enables the analysis of larger datasets. However, large datasets require massive computing power, which most platforms cannot support.

This study presents an approach to automated signal detection using LIDO's outputs. Initially, qualitative methods such as listening and visually inspection of spectrograms were used to classify animals' acoustic repertoires. This methodology involves systematically identifying peaks above the baseline level, which streamlines the data processing and allows for faster analysis. However, the absence of acoustic activity does not necessarily indicate the absence of animals, as some cetaceans may be present but not vocalizing. On the other hand, a higher density of detected cetacean vocalization could result from several factors, such as an increase in animal presence, a variation in the cue rate (due to behavioral or seasonal reasons), or reduced masking effects. The detector performance may be affected by masking and surrounding sounds. In any case, our study does not allow for a definitive assessment of the relative density of acoustically active species.

Adopting tools that enable long-term monitoring is crucial to establish a more effective legislative framework for conservation and noise regulation. Projects like LIDO serve as useful and valuable near-real-time recording platforms for inexperienced and advanced users. Facilitating easier access to large datasets allows bioacousticians to identify sounds in recordings through automatic detection and then, when aiming for a more specific goal, an in-depth targeted approach could be developed. The ongoing collection of baseline data over time is vital for understanding the environmental health of the oceans and the potential impacts of anthropogenic sounds on marine ecosystems [56]. We stress the importance of using tools that allow for acoustic long-term monitoring, automated detection of sounds, and big data handling in order to better design a legislative framework for mitigating noise impacts.

5. Conclusions

We investigated noise levels in thirteen observatories (eight stations from ONC Canada and four from the JAMSTEC network and OBSEA in the Mediterranean Sea). In five of them, animal presence was observed. The main conclusions of this study are:

- We found a yearly variability in SNB levels not significantly influenced by marine traffic, thus dominated by natural and biological patterns.
- In some locations, a drop in SNB levels can be expected during the first few months of the year as part of the usual variation in the sound levels, which recurs in a similar pattern each year.
- The SNB level (Figure 3, Supplementary Figure S1) showed an annual periodic trend with a seasonal near half-year cycle of decreasing followed by increasing levels for most locations (OBSEA, Barkley Canyon, Cascadia Basin, Clayoquot Slope, Endeavour, Vancouver Island, and all the Kushiro observatories).
- Since we analyzed data from hydrophones located far away from shipping lanes, our results showed that the halt in transportation due to COVID was not significant in terms of acoustic exposure at these locations.
- Three cetacean species were identified in the ONC observatories: humpback whales, orcas, and sperm whales. Our results drawn from ONC and the short tonal detector 10–45 Hz in JAMSTEC cannot provide a conclusive evaluation of the relative abundance of acoustically active species during the COVID period.
- The long-term methodology applied in this study has the potential to estimate trends in cetacean vocalization rate within the area.

Supplementary Materials: Supplementary figures and tables are included in the Supplementary material file. The following supporting information can be downloaded at: www.mdpi.com/xxx/s1, **Figure S1**: Shipping noise band daily median in : a) Barkley Canyon from 2018 to 2020, b) Cascadia Basin from 2017 to 2019, c) Endeavour from 2017 to 2020, d) Saanich Inlet in 2020, e) Strait of Georgia from 2016 and 2019, f) Vancouver Island from 2017 and 2019, g) Cambridge Bay from 2017 to 2019, h) Kushiro 2 from 2016 to 2018 and from 2020 to 2021, i) Kushiro 3 from 2016 to 2021 and j) Hatsushima from 2016 to 2017. Blue dots represent the daily median values, with colors transitioning from light to dark blue by year. The linear model fitted to each selected period by year is the red solid line and the dashed lines are the 95% confidence intervals; **Figure S2**: Slope distribution (one month lag) of shipping noise band daily median per year during the selected period in: a) Barkley Canyon b) Cascadia Basin, c) Endeavour, d) Strait of Georgia, e) Vancouver Island, f) Cambridge Bay, g) Kushiro 2, h) Kushiro 3 and i) Hatsushima. Individual observations on top of boxes were added by shifting all dots by a random value to avoid overlaps. The median comparison p-value of the pairwise Wilcoxon test is displayed on top of the box plots; **Figure S3**: Distribution of shipping noise band daily median per year in: a) Obsea, b) Clayoquot Slope, c) Kushiro 1, d) Barkley Canyon, e) Cascadia Basin, f) Endeavour, g) Strait of Georgia, h) Vancouver Island, i) Cambridge Bay, j) Kushiro 2, k) Kushiro 3 and l) Hatsushima. Individual observations on top of boxes were added by shifting all dots by a random value to avoid overlaps. The red dot represents the daily average. The median comparison p-value of the pairwise Wilcoxon test is displayed on top of the box plots; **Figure S4**: ROC curve of the Impulses 5000-20000 Hz detector for Endeavour in 2018; **Figure S5**: Smoothed indicator of the short tonal 1-2500 Hz detector for Barkley Canyon in 2019. The dashed line in red represents the selected threshold; **Figure S6**: Smoothed indicator of the short tonal 2500-20000 Hz detector for Barkley Canyon in 2019. The dashed line in red represents the selected threshold; **Figure S7**: Smoothed indicator of the short tonal 20000-46000 Hz detector for Barkley Canyon in 2019. The dashed line in red represents the selected threshold; **Figure S8**: Smoothed indicator of the impulses between 500-5000 Hz detector for Barkley Canyon in 2019. The dashed line in red represents the selected threshold; **Figure S9**: Smoothed indicator of the impulses between 5000-20000 Hz detector for Barkley Canyon in 2019. The dashed line in red represents the selected threshold; **Figure S10**: Smoothed indicator of the impulses between 20000-46000 Hz detector for Barkley Canyon in 2019. The dashed line in red represents the selected threshold; **Table S1**: Hydrophone deployment information, specific characteristics and recording time of all the locations analyzed; **Table S2**: P-values of the Shapiro-Wilk test of normality, applied to the slope SNB daily median distribution per year in all the LIDO locations with more than a year of data; **Table S3**: P-values of the one-way analysis of variance (ANOVA) comparing the means of the slope SNB daily median distribution per year for Clayoquot Slope Kushiro 1 and 2; **Table S4**: P-values of the t-test used to determine if there is a significant difference between the yearly means of two of the slopes SNB daily median distribution in all the LIDO locations where there is not the strong evidence to reject the normality assumption; **Table S5**: P-values of the Kruskal-Wallis test by ranks, a non-parametric method for testing whether yearly samples of the slope SNB daily median originate from the same distribution in all the LIDO locations with more than two years; **Table S6**: P-values of the Wilcoxon rank-sum test, a non-parametric method for comparing that the medians of the slope SNB daily median distribution of two years are equal; **Table S7**: P-values of the Kolmogorov-Smirnoff test, a non-parametric method for comparing the one-dimensional probability distributions of the yearly slope SNB daily median; **Table S8**: Results of the animal presence manual checking from January to April for each year and detector in Endeavour. The following abbreviations were used: Mn – Humpback whales (Megaptera novaeangliae), Oo - Killer whales (Orcinus orca), Pm - Sperm whales (Physeter macrocephalus), FP - False Positives and TN - True Negatives; **Table S9**: Selected thresholds for each year and detector in Barkley Canyon; **Table S10**: False positive rate for each detector with all year combined in Barkley Canyon; **Table S11**: Percentage of times an animal vocalization was above the selected threshold, corrected by the false positive rate, for each year and detector in Barkley Canyon; **Table S12**: Selected thresholds for each year and detector in Clayoquot Slope; **Table S13**: False positive rate for each detector with all year combined in Clayoquot Slope; **Table S14**: Percentage of times an animal vocalization was above the selected threshold, corrected by the false positive rate, for each year and detector in Clayoquot Slope; **Table S15**: Selected thresholds for each year and detector in Vancouver Island; **Table S16**: False positive rate for each detector with all year combined in Vancouver Island; **Table S17**: Percentage of times an animal vocalization was above the selected threshold, corrected by the false positive rate, for each year and detector in Vancouver Island; **Table S18**: Selected thresholds for the short tonal 10 - 45 Hz detector each year in Kushiro 1; **Table S19**: False positive rate for the short tonal 10 - 45 Hz detector with all year combined in Kushiro 1; **Table S20**: Percentage of times an animal vocalization was above the selected threshold, corrected by the false positive rate, for the short tonal 10 - 45 Hz detector for each year in Kushiro 1.

Author Contributions: Conceptualization, R.P.G., A.A., M.v.d.S. and M.A.; methodology, R.P.G. and M.v.d.S.; formal analysis, R.P.G., A.A. and M.v.d.S.; investigation, R.P.G. and A.A.; resources, M.v.d.S. and M.A.; data curation, R.P.G. and M.v.d.S.; writing—original draft preparation, R.P.G. and A.A.; writing—review and editing, R.P.G., A.A., M.v.d.S. and M.A; visualization, R.P.G. and A.A. All authors have read and agreed to the published version of the manuscript.

Funding: A.A. is currently funded by the National Institute of Oceanography and Applied Geophysics—OGS, the University of Trieste, and JASCO Applied Sciences. During the early stages of this study, A.A. was funded by the Deep Blue project coordinated by OGS ICAP—Developing Education and Employment Partnerships for a Sustainable Blue Growth in the Western Mediterranean Region (European Maritime and Fishery Fund and European Agency for Small and Medium-sized enterprises within the framework of the Sustainable Blue Economy Call 2017 (EASME/EMFF/2017/1.2.1.12/S3/02/SI2.789633).

Data Availability Statement: The acoustic recordings data used in the analysis for ONC and JAMSTEC are freely downloadable from the websites: ONC; www.oceannetworks.ca (accessed on 20 November 2024) and JAMSTEC, www.jamstec.go.jp (accessed on 20 November 2024). The LIDO platform can be explored at http://listentothedeep.com/acoustics/ accessed on 20 November 2024.

Conflicts of Interest: Rocío Prieto González is the founder and sole employee of the company Counting Whales. The remaining authors declare that the research was conducted in the absence of any commercial or financial relationships that could be construed as a potential conflict of interest. The authors declare no conflicts of interest. The funders had no role in the design of the study; in the collection, analyses, or interpretation of data; in the writing of the manuscript; or in the decision to publish the results.

References

1. Trisos, C.H.; Merow, C.; Pigot, A.L. The projected timing of abrupt ecological disruption from climate change. *Nature* **2020**, *580*, 496–501. https://doi.org/10.1038/s41586-020-2189-9.
2. Mehvar, S.; Filatova, T.; Dastgheib, A.; De Ruyter van Steveninck, E.; Ranasinghe, R. Quantifying economic value of coastal ecosystem services: A review. *J. Mar. Sci. Eng.* **2018**, *6*, 5. https://doi.org/10.3390/jmse6010005.
3. Duarte, C.M.; Chapuis, L.; Collin, S.P.; Costa, D.P.; Devassy, R.P.; Eguiluz, V.M.; Erbe, C.; Gordon, T.A.C.; Halpern, B.S.; Harding, H.R.; et al. The soundscape of the anthropocene ocean. *Science* **2021**, *371*, eaba4658. https://doi.org/10.1126/science.aba4658.
4. Halpern, B.S.; Walbridge, S.; Selkoe, K.A.; Kappel, C.V.; Micheli, F.; D'Agrosa, C.; Bruno, J.F.; Casey, K.S.; Ebert, C.; Fox, H.E.; et al. A global map of human impact on marine ecosystems. *Science* **2018**, *319*, 948–952. https://doi.org/10.1126/science.1149345.
5. Wilson, K.A.; Auerbach, N.A.; Sam, K.; Magini, A.G.; Moss, A.S.L.; Langhans, S.D.; Budiharta, S.; Terzano, D.; Meijaard, E. Conservation research is not happening where it is most needed. *PLoS Biol.* **2016**, *14*, e1002413. https://doi.org/10.1371/journal.pbio.1002413.
6. Jones, N. Ocean uproar: Saving marine life from a barrage of noise. *Nature* **2019**, *568*, 158–162.
7. Andrew, R.K.; Howe, B.M.; Mercer, J.A.; Dzieciuch, M.A. Ocean ambient sound: Comparing the 1960s with the 1990s for a receiver off the california coast. *Acoust. Res. Lett. Online* **2002**, *3*, 65–70. https://doi.org/10.1121/1.1461915.
8. National Research Council; Division on Earth, Life Studies, Ocean Studies Board; Committee on Potential Impacts of Ambient Noise in the Ocean on Marine Mammals. *Ocean Noise and Marine Mammals*; National Academies Press: Washington, DC, USA, 2003. https://doi.org/10.17226/10564.
9. McKenna, M.F.; Shannon, G.; Fristrup, K. Characterizing anthropogenic noise to improve understanding and management of impacts to wildlife. *Endanger. Species Res.* **2016**, *31*, 279–291. https://doi.org/10.1121/1.5137190.
10. Miksis-Olds, J.L.; Nichols, S.M. Is low frequency ocean sound increasing globally? *J. Acoust. Soc. Am.* **2016**, *139*, 501–511. https://doi.org/10.1121/1.4938237.
11. Popper, A.N.; Hastings, M. The effects of anthropogenic sources of sound on fishes. *J. Fish Biol.* **2009**, *75*, 455–489. https://doi.org/10.1111/j.1095-8649.2009.02319.x.
12. Weilgart, L.S. The impacts of anthropogenic ocean noise on cetaceans and implications for management. *Can. J. Zool.* **2007**, *85*, 1091–1116. https://doi.org/10.1139/Z07-101.
13. Fournet, M.E.; Matthews, L.P.; Gabriele, C.M.; Haver, S.; Mellinger, D.K.; Klinck, H. Humpback whales Megaptera novaeangliae alter calling behavior in response to natural sounds and vessel noise. *Mar. Ecol. Prog. Ser.* **2018**, *607*, 251–268. https://doi.org/10.3354/meps12784.
14. McKenna, M.F.; Ross, D.; Wiggins, S.M.; Hildebrand, J.A. Underwater radiated noise from modern commercial ships. *J. Acoust. Soc. Am.* **2012**, *131*, 92–103. https://doi.org/10.1121/1.3664100.

15. McKenna, M.F.; Gabriele, C.; Kipple, B. Effects of marine vessel management on the underwater acoustic environment of glacier bay national park. *Ocean Coast. Manag.* **2017**, *139*, 102–112. https://doi.org/10.1016/j.ocecoaman.2017.01.015.
16. Haver, S.M.; Klinck, H.; Nieukirk, S.L.; Matsumoto, H.; Dziak, R.P.; Miksis-Olds, J.L. The not-so-silent world: Measuring arctic, equatorial, and antarctic soundscapes in the atlantic ocean. *Deep Sea Res. I Oceanogr. Res. Pap.* **2017**, *122*, 95–104 https://doi.org/10.1016/j.dsr.2017.03.002.
17. Rutz, C.; Loretto, M.C.; Bates, A.E.; Davidson, S.C.; Duarte, C.M.; Jetz, W.; Johnson, M.; Kato, A.; Kays, R.; Mueller, T.; et al. COVID-19 lockdown allows researchers to quantify the effects of human activity on wildlife. *Nat. Ecol. Evol.* **2020**, *4*, 1156–1159. https://doi.org/10.1016/j.biocon.2021.109175.
18. March, D.; Metcalfe, K.; Tintoré, J.; Godley, B.J. Tracking the global reduction of marine traffic during the covid-19 pandemic. *Nat. Commun.* **2021**, *12*, 2415. https://doi.org/10.1038/s41467-021-22423-6.
19. Millefiori, L.M.; Braca, P.; Zissis, D.; Spiliopoulos, G.; Marano, S.; Willett, P.K.; Carniel, S. COVID-19 impact on global maritime mobility. *Sci. Rep.* **2021**, *11*, 18039. https://doi.org/10.1038/s41598-021-97461-7.
20. Breeze, H.; Li, S.; Marotte, E.C.; Theriault, J.A.; Wingfield, J.; Xu, J. Changes in underwater noise and vessel traffic in the approaches to Halifax Harbor, Nova Scotia, Canada. *Front. Mar. Sci.* **2021**, *8*, 674788. https://doi.org/10.3389/fmars.2021.674788.
21. Depellegrin, D.; Bastianini, M.; Fadini, A.; Menegon, S. The effects of COVID-19 induced lockdown measures on maritime settings of a coastal region. *Sci. Total Environ.* **2020**, *740*, 140123. https://doi.org/10.1016/j.scitotenv.2020.140123.
22. Gabriele, C.M.; Ponirakis, D.W.; Klinck, H. Underwater sound levels in Glacier Bay during reduced vessel traffic due to the COVID-19 pandemic. *Front. Mar. Sci* **2021**, *8*, 674787. https://doi.org/10.3389/fmars.2021.674787.
23. Basan, F.; Fischer, J.G.; Kühnel, D. Soundscapes in the German Baltic Sea before and during the COVID-19 pandemic. *Front. Mar. Sci.* **2021**, *8*, 689860. https://doi.org/10.3389/fmars.2021.689860.
24. Derryberry, E.P.; Phillips, J.N.; Derryberry, G.E.; Blum, M.J.; Luther, D. Singing in a silent spring: Birds respond to a half-century soundscape reversion during the COVID-19 shutdown. *Science* **2020**, *370*, 575–579. https://doi.org/10.1126/science.abd5777.
25. Pine, M.K.; Wilson, L.; Jeffs, A.G.; McWhinnie, L.; Juanes, F.; Scuderi, A.; Radford, C.A. A Gulf in lockdown: How an enforced ban on recreational vessels increased dolphin and fish communication ranges. *Glob. Change Biol*. **2021**, *27*, 4839–4848. https://doi.org/10.1111/gcb.15798.
26. Ryan, J.P.; Joseph, J.E.; Margolina, T.; Hatch, L.T.; Azzara, A.; Reyes, A.; Southall, B.L.; DeVogelaere, A.; Reeves, L.E.P.; Zhang, Y.; et al. Reduction of low-frequency vessel noise in Monterey Bay National Marine Sanctuary during the COVID-19 pandemic. *Front. Mar. Sci.* **2021**, *8*, 656566. https://doi.org/10.3389/fmars.2021.656566.
27. Thomson, D.J.; Barclay, D.R. Real-time observations of the impact of covid-19 on underwater noise. *J. Acoust. Soc. Am.* **2020**, *147*, 3390–3396. https://doi.org/10.1121/10.0001271.
28. Dunn, C.; Theriault, J.; Hickmott, L.; Claridge, D. Slower ship speed in the Bahamas due to COVID-19 produces a dramatic reduction in ocean sound levels. *Front. Mar. Sci.* **2021**, *8*, 673565. https://doi.org/10.3389/fmars.2021.673565.
29. Bertucci, F.; Lecchini, D.; Greeven, C.; Brooker, R.M.; Minier, L.; Cordonnier, S.; René-Trouillefou, M.; Parmentier, E. Changes to an urban marina soundscape associated with COVID-19 lockdown in Guadeloupe. *Environ. Pollut.* **2021**, *289*, 117898. https://doi.org/10.1016/j.envpol.2021.117898.
30. Gagne, E.; Perez-Ortega, B.; Hendry, A.P.; Melo-Santos, G.; Walmsley, S.F.; Rege-Colt, M.; Austin, M.; May-Collado, L.J. Dolphin communication during widespread systematic noise reduction-a natural experiment amid COVID-19 lockdowns. *Front. Remote Sens.* **2022**, *3*, 934608.
31. Albouy, C.; Delattre, V.; Donati, G.; Frölicher, T.L.; Albouy-Boyer, S.; Rufino, M.; Pellissier, L.; Mouillot, D.; Leprieur, F. Global vulnerability of marine mammals to global warming. *Sci. Rep.* **2020**, *10*, 548. https://doi.org/10.1038/s41598-019-57280-3.
32. Bearzi, M. Cetaceans and MPAs should go hand in hand: A case study in Santa Monica Bay, California. *Ocean Coast. Manag.* **2012**, *60*, 56. https://doi.org/10.1016/j.ocecoaman.2011.12.019.
33. Lusseau, D.; Bain, D.E.; Williams, R.; Smith, J.C. Vessel traffic disrupts the foraging behavior of southern resident killer whales Orcinus orca. *Endanger. Species Res.* **2009**, *6*, 211–221. https://doi.org/10.3354/esr00154.
34. Ward, E.J.; Ford, M.J.; Kope, R.G.; Ford, J.K.; Vélez-Espino, L.A.; Parken, C.K.; LaVoy, L.; Hanson, M.B.; Balcomb, K.C. Estimating the impacts of Chinook salmon abundance and prey removal by ocean fishing on Southern Resident killer whale population dynamics. In *U.S. Dept. Commer., NOAA Tech. Memo. NMFS-NWFSC-123*, 2013.
35. Available online: http://listentothedeep.com (accessed on 18 November 2024).
36. André, M.; van der Schaar, M.; Zaugg, S.; Houégnigan, L.; Sánchez, A.; Castell, J. Listening to the deep: Live monitoring of ocean noise and cetacean acoustic signals. *Mar. Pollut. Bull.* **2021**, *63*, 18–26. https://doi.org/10.1016/j.marpolbul.2011.04.038.
37. R Core Team. *R: A Language and Environment for Statistical Computing*; version 4.0.2; R Foundation for Statistical Computing: Vienna, Austria, 2021. Available online: https://www.R-project.org/
38. Python Software Foundation. Python Language Reference, Version 3.7.3. Available online: https://www.python.org
39. Wang, L.; Ward, J.; Robinson, S. Standard for Data Processing of Measured Data (Draft). Report of the EU INTERREG Joint Monitoring Programme for Ambient Noise North Sea (JOMOPANS). 2019. Available online: https://northsearegion.eu/jomopans/output-library/ (accessed on 21 June 2020).
40. Prieto González, R.; van der Schaar, M.; André, M. Deliverable 8.1: Utilising bioacoustic data as a proxy for biodiversity/ecosystem health monitoring. In *Joint Framework for Ocean Noise in the Atlantic Seas (JONAS) EAPA_52/2018*, 2022.

41. Longden, E.G.; Gillespie, D.; Mann, D.A.; McHugh, K.A.; Rycyk, A.M.; Wells, R.S.; Tyack, P.L. Comparison of the marine soundscape before and during the COVID-19 pandemic in dolphin habitat in Sarasota Bay, FL. *J. Acoust. Soc. Am.* **2022**, *152*, 3170–3185. https://doi.org/10.1121/10.0015366.
42. Miksis-Olds, J.L.; Martin, B.S.; Lowell, K.; Verlinden, C.; Heaney, K.D. Minimal COVID-19 quieting measured in the deep offshore waters of the US Outer Continental Shelf. *JASA Express Lett.* **2022**, 2, 090801. https://doi.org/10.1121/10.0013999.
43. McDonald, M.A.; Hildebrand, J.A.; Wiggins, S.M. Increases in deep ocean ambient noise in the northeast pacific west of san nicolas island, California. *J. Acoust. Soc. Am.* **2006**, *120*, 711–718. https://doi.org/10.1121/1.2216565.
44. Vagle, S.; Burnham, R.E.; O'neill, C.; Yurk, H. Variability in anthropogenic underwater noise due to bathymetry and sound speed characteristics. *J. Mar. Sci. Eng.* **2021**, *9*, 1047. https://doi.org/10.3390/jmse9101047.
45. Mustonen, M.; Klauson, A.; Andersson, M.; Clorennec, D.; Folegot, T.; Koza, R.; Pajala, J.; Persson, L.; Tegowski, J.; Tougaard, J.; et al. Spatial and temporal variability of ambient underwater sound in the baltic sea. *Sci. Rep.* **2019**, *9*, 13237. https://doi.org/10.1038/s41598-019-48891-x.
46. Klusek, Z.; Lisimenka, A. Seasonal and diel variability of the underwater noise in the Baltic Sea. *J. Acoust. Soc. Am.* **2016**, *139*, 1537–1547. https://doi.org/10.1121/1.4944875.
47. Parsons, E.; Baulch, S.; Bechshoft, T.; Bellazzi, G.; Bouchet, P.; Cosentino, A.; Godard-Codding, C.; Gulland, F.; Hoffmann-Kuhnt, M.; Hoyt, E.; et al. Key research questions of global importance for cetacean conservation. *Endanger. Species Res.* **2015**, *27*, 113–118. https://doi.org/10.3354/esr00655.
48. Tort Castro, B.; Prieto Gonzalez, R.; O'Callaghan, S.A.; Dominguez Rein-Loring, P.; Degollada Bastos, E. Ship Strike Risk for Fin Whales (*Balaenoptera physalus*) Off the Garraf coast, Northwest Mediterranean Sea. *Front. Mar. Sci.* **2022**, *9*, 867287. https://doi.org/10.3389/fmars.2022.867287.
49. Bejder, L.; Samuels, A.; Whitehead, H.; Gales, N.; Mann, J.; Connor, R.; Heithaus, M.; Watson-Capps, J.; Flaherty, C.; Krützen, M. Decline in relative abundance of bottlenose dolphins exposed to long-term disturbance. *Conserv. Biol.* **2006**, *20*, 1791–1798. https://doi.org/10.1111/j.1523-1739.2006.00540.x.
50. Lusseau, D. Residency pattern of bottlenose dolphins Tursiops spp. in Milford Sound, New Zealand, is related to boat traffic. *Mar. Ecol. Prog. Ser.* **2005**, *295*, 265–272. https://doi.org/10.3354/meps295265.
51. van der Schaar, M.; Zaugg, S.; André, M. Sounds in Japan's deep: Long-term monitoring of fin whales. *ECO Spec. Issue Ocean. Sound* **2019**, 52–55.
52. Oleson EM, Širović A, Bayless AR, et al Synchronous seasonal change in fin whale song in the north pacific. *PLoS ONE* **2014**, *9*, e115678. https://doi.org/10.1371/journal.pone.0115678.
53. Širović, A.; Oleson, E.M.; Buccowich, J.; Rice, A.; Bayless, A.R. Fin whale song variability in southern California and the Gulf of California. *Sci. Rep.* **2017**, *7*, 10126. https://doi.org/10.1038/s41598-017-09979-4.
54. Sugioka, H.; Kyo, M.; Yoshida, R.; Yamada, H.; Kato, H. Detection and characterization of whale signals using seafloor cabled seismic networks offshore Japan. In Proceedings of the OCEANS 2015-MTS/IEEE Washington, Washington, DC, USA, 19–22 October 2015; IEEE: Piscataway, NJ, USA, 2015; pp. 1–7. https://doi.org/10.23919/OCEANS.2015.7404452.
55. Buchan, S.; Gutierrez, L.; Balcazar-Cabrera, N.; Stafford, K. Seasonal occurrence of fin whale song off juan fernandez, chile. *Endanger. Species Res.* **2019**, *39*, 135–145. https://doi.org/10.3354/esr00956.
56. Tyack, P.L.; Miksis-Olds-Olds, J.; Urban, E.R., Jr.; Ausubel, J. Measuring ambient ocean sound during the COVID-19 pandemic. *Eos* **2021**, *102*. https://doi.org/10.1029/2021EO155447.